Journal of Computing and Electronic Information Management
ISSN: 2413-1660 | Vol. 10, No. 1, 2023

Kinematics analysis and simulation of 2-CRS-S' parallel mechanism

Xianhui Tan[1,2,3], Wei Li [1,2,3,*], Quan Fu [1,2,3], Xianchen Zhou [1,2,3], Kunyang Yuan [1,2,3], Lei Mou [1,2,3], Depeng Lai [1,2,3]

[1]College of Mechanical and Electrical Engineering, Southwest Petroleum University, Chengdu 610500, China
[2] Key Laboratory of Oil and Gas Equipment, Ministry of Education, Southwest Petroleum University, Chengdu 610500, China
[3] Energy Equipment Research Institute, Southwest Petroleum University, Chengdu 610500, China
[*] **Corresponding author**: Wei Li

Abstract: A 2-CRS-S ' parallel mechanism is proposed in this paper. The parallel mechanism consists of a static platform, two identical driving branches, a moving platform and a fixed branch, with two rotational degrees of freedom on the X and Y axes. Taking the driving branch chain in the mechanism as the research object, the inverse kinematics analysis of the parallel mechanism is carried out by using the D-H analysis method, and on this basis, the forward kinematics analysis of the structure is carried out by combining the particle swarm optimization algorithm. Finally, the Adams software is used to simulate and analyze the mechanism, and the motion angle curve of the moving platform of the mechanism is obtained, which verifies the correctness of the theoretical analysis. The obtained motion angle curves show regular periodic changes, and the curves have no breakpoints and mutations, indicating that the mechanism runs smoothly during the movement and has good kinematic performance.

Keywords: Parallel mechanism; Theory of D-H analysis; Particle swarm optimization.

1. Introduction

Parallel mechanism is a new type of mechanism, which has incomparable advantages over traditional serial mechanism. It is the supplement and extension of serial mechanism and plays an important role in machine tool technology and robot technology.

With the advantages of stable structure and smooth operation, the parallel mechanism is widely used in all walks of life, which improves the working efficiency, reduces the interference of human factors in the working process, and improves the accuracy and stability in the automatic production process. In parallel mechanisms, parallel mechanisms with fewer degrees of freedom tend to have simpler structures, fewer constraints, lower possibility of mutual interference between components, and lower control difficulty. Zhu Dongsheng et al. analyzed the kinematics of 4-SPS / UPU parallel mechanism. The degree of freedom of the mechanism was analyzed by screw theory, and the forward and inverse kinematics solutions were derived. After establishing the workspace constraint conditions, the numerical analysis was carried out by MATLAB software, and the working position of the mechanism under fixed attitude was solved. Chen Wenbo et al. take a 2UPR / UPS / UP redundant parallel mechanism with three degrees of freedom in space as the research object, carry out relevant kinematics analysis and mechanical analysis, obtain the change rule of each driving branch chain and establish the dynamic analysis model of the mechanism, and then verify the correctness of the kinematics and dynamics model through simulation analysis. Zou Yupen et al. proposed an ankle joint robot based on a 3-RRS parallel mechanism. The spherical analytical theory was used to analyze the motion characteristics of the parallel mechanism. The screw theory was used to solve the degree of freedom of the parallel mechanism. The trajectory of the mechanism was planned and the accuracy of the kinematics model was verified by virtual prototype simulation.

In this paper, the 2-CRS-S' parallel mechanism is taken as the research object. Firstly, the modified G-K formula is used to calculate the degree of freedom of the parallel mechanism, and then the D-H theoretical analysis method is used to solve the inverse kinematics of the parallel mechanism [10]. Combined with the inverse solution equation and the particle swarm optimization algorithm, the forward kinematics optimization solution of the parallel mechanism is carried out. Finally, the kinematics analysis of the 2-CRS-S' parallel mechanism is carried out by Adams virtual prototype, and the motion characteristics of the parallel mechanism are explored, which provides a theoretical basis for the application of the mechanism in the automation industry.

2. Structure description of 2-CRS-S ' parallel mechanism

The spatial model of the 2-CRS-S ' parallel mechanism is shown in Figure 1, which can be regarded as a static platform, two identical drive branches, a moving platform and a fixed branch. Each drive branch is composed of a cylindrical pair C, a rotary pair R and a spherical hinge pair S ', and each drive branch is evenly distributed 120 degrees apart. It is connected to the moving platform through the spherical hinge pair S ', to the static platform through the cylindrical pair C, and to the moving platform through the ball pin pair.

In this paper, the modified Kutzbach-Grubler formula is used to calculate the degree of freedom of the mechanism. The calculation formula is as follows:

$$M = 6(N - p - 1) + \sum_{i=1}^{p} f_i + \lambda - \xi \quad (1)$$

In the formula, M is the number of degrees of freedom of the mechanism; N is the number of components in the mechanism (including the frame); p is the number of kinematic pairs; fi is the degree of freedom of the i th motion

pair; λ is the number of redundant constraints of the parallel mechanism after removing the factors of common constraints; ξ is the number of local degrees of freedom in the mechanism.

In this mechanism, the number of components N is 8, the number of kinematic pairs p is 10, the number of redundant constraints λ is 0, the number of local degrees of freedom ξ is 0, the degree of freedom of the cylindrical pair is 2, the degree of freedom of the rotating pair is 1, the degree of freedom of the ball pin pair is 2, and the degree of freedom of the ball hinge pair is 3.

By substituting all the parameters into the formula, the degree of freedom M of the 2-CRS-S ' parallel mechanism is calculated to be 2.

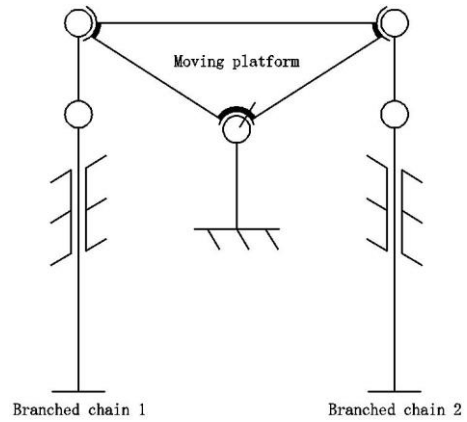


Fig.1 Structure diagram of 2-CRS-S ' parallel mechanism

3. Inverse solution analysis of motion based on D-H analysis method

In order to describe the position and attitude of the 2-CRS-S ' parallel mechanism in space in more detail, this paper uses the D-H analysis method to establish a coordinate system at each joint point in the parallel, as shown in Figure 2, in which the D-H parameters on the two driving branches are consistent [11], as shown in Table 1.

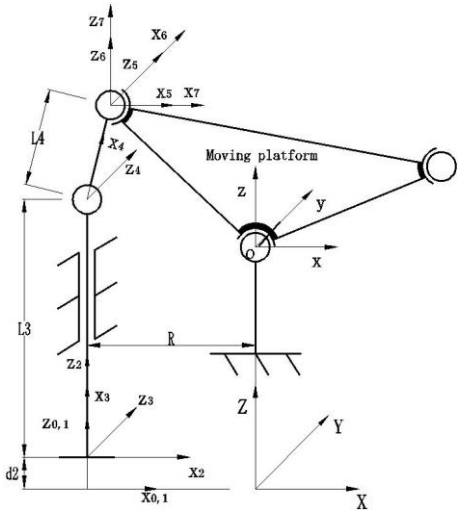


Fig.2 Establishment of D-H coordinate system of driving branch chain

In Table 1, αi-1 is the degree of rotation from Zi-1 to Zi around the Xi-1 axis; αi-1 is the distance from Zi-1 to Zi along the Xi-1 axis. θi is the rotation degree from Xi-1 to Xi around Zi axis; di is the length from Xi-1 to Xi along the Zi axis. In Table 1, L3 and L4 are constants (L3 is the distance from the center point of the cylindrical pair C on the driving branched chain to the center point of the revolute pair R, L4 is the length from the center point of the revolute pair R to the center point of the ball pin pair S), and θ1, d2, θ4, θ5,6 and θ7 are variables generated by the movement of the mechanism.

Table.1 Driving branch chain D-H parameters

i	αi-1/(°)	ai-1/(mm)	θ	di
1	0	0	θ1	0
2	0	0	0	d2
3	-90°	0	-90°	0
4	0	L3	θ4	0
5	0	L4	θ5	0
6	90°	0	θ6	0
7	0	0	θ7	0

The general formula of matrix transformation between two adjacent coordinate systems { i } and { i-1 } in D-H analysis is :

$$ {}^{i-1}_{i}T = \begin{bmatrix} \cos\theta_i & -\sin\theta_i & 0 & a_{i-1} \\ \sin\theta_i\cos\alpha_{i-1} & \cos\theta_i\cos\alpha_{i-1} & -\sin\alpha_{i-1} & -d_i\sin\alpha_{i-1} \\ \sin\theta_i\sin\alpha_{i-1} & \cos\theta_i\sin\alpha_{i-1} & \cos\alpha_{i-1} & d_i\cos\alpha_{i-1} \\ 0 & 0 & 0 & 1 \end{bmatrix} \quad (2) $$

By substituting the D-H parameters of the driving branched chain in Table 1 into the formula (2), the transformation matrix between the coordinate systems can be obtained :

$$ {}^{0}_{1}T = \begin{pmatrix} \cos\theta_1 & -\sin\theta_1 & 0 & 0 \\ \sin\theta_1 & \cos\theta_1 & 0 & 0 \\ 0 & 0 & 1 & 0 \\ 0 & 0 & 0 & 1 \end{pmatrix}, $$

$$ {}^{1}_{2}T = \begin{pmatrix} 1 & 0 & 0 & 0 \\ 0 & 1 & 0 & 0 \\ 0 & 0 & 1 & d_2 \\ 0 & 0 & 0 & 1 \end{pmatrix} {}^{2}_{3}T = \begin{pmatrix} 0 & 1 & 0 & 0 \\ 0 & 0 & 1 & 0 \\ 1 & 0 & 0 & 0 \\ 0 & 0 & 0 & 1 \end{pmatrix}, $$

$$ {}^{3}_{4}T = \begin{pmatrix} \cos\theta_4 & -\sin\theta_4 & 0 & l_3 \\ \sin\theta_4 & \cos\theta_4 & 0 & 0 \\ 0 & 0 & 1 & 0 \\ 0 & 0 & 0 & 1 \end{pmatrix}, $$

$$ {}^{4}_{5}T = \begin{pmatrix} \cos\theta_5 & -\sin\theta_5 & 0 & l_4 \\ \sin\theta_5 & \cos\theta_5 & 0 & 0 \\ 0 & 0 & 1 & 0 \\ 0 & 0 & 0 & 1 \end{pmatrix}, $$

$$ {}^{5}_{6}T = \begin{pmatrix} \cos\theta_6 & -\sin\theta_6 & 0 & 0 \\ 0 & 0 & -1 & 0 \\ \sin\theta_6 & \cos\theta_6 & 0 & 0 \\ 0 & 0 & 0 & 1 \end{pmatrix}, $$

$$ {}^{6}_{7}T = \begin{pmatrix} \cos\theta_7 & -\sin\theta_7 & 0 & 0 \\ \sin\theta_7 & \cos\theta_7 & 0 & 0 \\ 0 & 0 & 1 & 0 \\ 0 & 0 & 0 & 1 \end{pmatrix} \quad (3) $$

The transformation matrix between the above coordinate systems is applicable to any drive branch chain in this offset mechanism. In the subsequent calculation, in order to facilitate the distinction, the branch chain prefix is added before the coordinate system name and variable parameter name in the drive branch chain. For example, in the branch chain 1, the coordinate system O0-x0y0z0 is denoted by O10-

x10y10z10, the coordinate system O1-x1y1z1 is denoted by O11-x11y11z11, and the coordinate system, the angle variable θ1 is denoted by θ11, and the displacement variable d2 is denoted by d12.

Therefore, the homogeneous transformation matrix from the coordinate system O10-x10y10z10 to the coordinate system O11-x11y11z11 is recorded as:

$$ {}^{0}_{1}T = \begin{pmatrix} \cos\theta_1 & -\sin\theta_1 & 0 & 0 \\ \sin\theta_1 & \cos\theta_1 & 0 & 0 \\ 0 & 0 & 1 & 0 \\ 0 & 0 & 0 & 1 \end{pmatrix} = {}^{10}_{11}T = \begin{pmatrix} \cos\theta_{11} & -\sin\theta_{11} & 0 & 0 \\ \sin\theta_{11} & \cos\theta_{11} & 0 & 0 \\ 0 & 0 & 1 & 0 \\ 0 & 0 & 0 & 1 \end{pmatrix} $$

After obtaining the transformation matrix between the coordinate systems in the driving branch chain, it is necessary to solve the transformation matrix between the dynamic coordinate system o-xyz to the end coordinate system O7-x7y7z7 of the driving branch chain and the initial coordinate system O0-x0y0z0 of the driving branch chain to the fixed coordinate system O-XYZ. The position relationship between the dynamic coordinate system o-xyz of the mechanism and the end coordinate system O7-x7y7z7 (O17-x17y17z17, O27-x27y27z27) of the driving branch chain is shown in Figure 3. The positional relationship between the fixed coordinate system O-XYZ of the mechanism and the initial coordinate system O0-x0y0z0 (O10-x10y10z10, O20-x20y20z20) of the driving branched chain is shown in Figure 4.

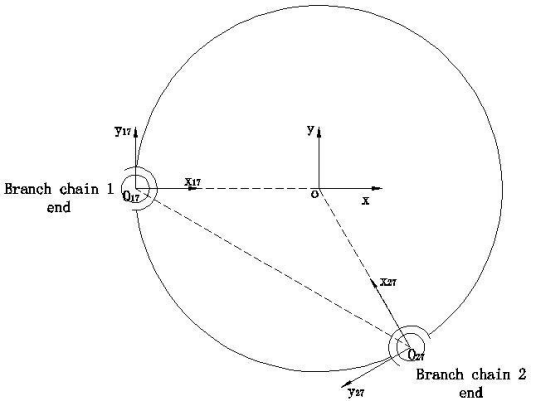


Fig.3 The positional relationship between the moving coordinate system and the end coordinate system of the driving branch chain

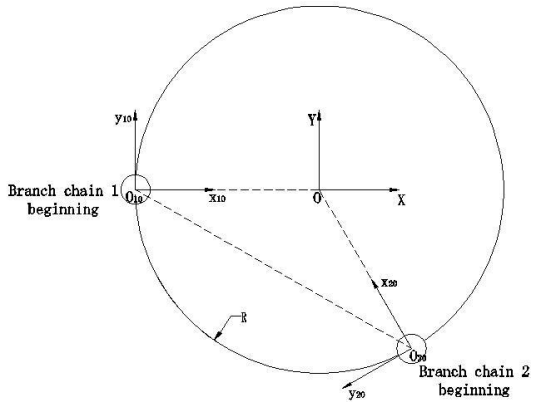


Fig.4 The positional relationship between the initial coordinate system and the fixed coordinate system of the driving branch chain

The transformation matrix from the end coordinate system O17-x17y17z17 of the driving branch 1 to the dynamic coordinate system o-xyz of the mechanism can be obtained as:

$$ {}^{17}_{o}T = \begin{pmatrix} 1 & 0 & 0 & R \\ 0 & 1 & 0 & 0 \\ 0 & 0 & 1 & 0 \\ 0 & 0 & 0 & 1 \end{pmatrix} \tag{4} $$

The transformation matrix from the fixed coordinate system O-XYZ of the mechanism to the initial coordinate system O10-x10y10z10 in the driving limb 1 can be obtained as:

$$ {}^{O}_{10}T = \begin{pmatrix} 1 & 0 & 0 & -R \\ 0 & 1 & 0 & 0 \\ 0 & 0 & 1 & 0 \\ 0 & 0 & 0 & 1 \end{pmatrix} \tag{5} $$

The transformation matrix from the end coordinate system O27-x27y27z27 in the driving branch 2 to the dynamic coordinate system o-xyz of the mechanism can be obtained as:

$$ {}^{27}_{o}T = \begin{pmatrix} -\frac{1}{2} & \frac{\sqrt{3}}{2} & 0 & R \\ -\frac{\sqrt{3}}{2} & -\frac{1}{2} & 0 & 0 \\ 0 & 0 & 1 & 0 \\ 0 & 0 & 0 & 1 \end{pmatrix} \tag{6} $$

The transformation matrix from the fixed coordinate system O-XYZ of the mechanism to the initial coordinate system O20-x20y20z20 in the driving branch 2 is obtained as follows:

$$ {}^{O}_{20}T = \begin{pmatrix} -\frac{1}{2} & -\frac{\sqrt{3}}{2} & 0 & \frac{R}{2} \\ \frac{\sqrt{3}}{2} & -\frac{1}{2} & 0 & -\frac{\sqrt{3}}{2}R \\ 0 & 0 & 1 & 0 \\ 0 & 0 & 0 & 1 \end{pmatrix} \tag{7} $$

R is the radius from the fixed platform / moving platform to the circumcircle of the mechanism (the size of the moving platform and the fixed platform of the mechanism is the same, so the radius of the two is equal).

Combined with the transformation relationship of each coordinate system in the mechanism, the calculation formula of the transformation matrix of the dynamic coordinate system o-xyz relative to the fixed coordinate system O-XYZ is as follows:

$$ {}^{O}_{o}T_1 = {}^{O}_{10}T\,{}^{10}_{11}T\,{}^{11}_{12}T\,{}^{12}_{13}T\,{}^{13}_{14}T\,{}^{14}_{15}T\,{}^{15}_{16}T\,{}^{16}_{17}T\,{}^{17}_{o}T = \begin{bmatrix} M_{11} & M_{12} & M_{13} & M_{14} \\ M_{21} & M_{22} & M_{23} & M_{24} \\ M_{31} & M_{32} & M_{33} & M_{34} \\ 0 & 0 & 0 & 1 \end{bmatrix} \tag{8} $$

$$ \begin{aligned} M_{11} &= -\cos\theta_{17}\left(\sin\theta_{11}\sin\theta_{16} - \cos\theta_{11}\cos\theta_{16}\sin\left(\theta_{14}+\theta_{15}\right)\right) \\ &\quad -\sin\theta_{17}\left(\cos\theta_{11}\sin\theta_{16}\sin\left(\theta_{14}+\theta_{15}\right)+\sin\theta_{11}\cos\theta_{16}\right) \\ M_{12} &= \sin\theta_{17}\left(\sin\theta_{11}\sin\theta_{16} - \cos\theta_{11}\cos\theta_{16}\sin\left(\theta_{14}+\theta_{15}\right)\right) \\ &\quad -\cos\theta_{17}\left(\cos\theta_{11}\sin\theta_{16}\sin\left(\theta_{14}+\theta_{15}\right)+\sin\theta_{11}\cos\theta_{16}\right) \\ M_{13} &= cos\,\theta_{11}\,sin(\theta_{14}+\theta_{15}) \end{aligned} $$

$$M_{14}=L_4\cos\theta_{11}\sin\theta_{14}-R\begin{pmatrix}\cos\theta_{17}\left(\sin\theta_{11}\sin\theta_{16}-\cos\theta_{11}\cos\theta_{16}\sin\left(\theta_{14}+\theta_{15}\right)\right)\\+\sin\theta_{17}\left(\cos\theta_{11}\sin\theta_{16}\sin\left(\theta_{14}+\theta_{15}\right)+\sin\theta_{11}\cos\theta_{16}\right)\end{pmatrix}-R$$
$$-L_7\cos\theta_{11}\cos\left(\theta_{14}+\theta_{15}\right)$$
$$M_{21}=\cos\theta_{17}\left(\sin\theta_{11}\cos\theta_{16}\sin\left(\theta_{14}+\theta_{15}\right)-\cos\theta_{11}\sin\theta_{16}\right)$$
$$-\sin\theta_{17}\left(\sin\theta_{11}\sin\theta_{16}\sin\left(\theta_{14}+\theta_{15}\right)-\cos\theta_{11}\cos\theta_{16}\right)$$
$$M_{22}=-\sin\theta_{17}\left(\sin\theta_{11}\cos\theta_{16}\sin\left(\theta_{14}+\theta_{15}\right)+\cos\theta_{11}\sin\theta_{16}\right)$$
$$-\cos\theta_{17}\left(\sin\theta_{11}\sin\theta_{16}\sin\left(\theta_{14}+\theta_{15}\right)-\cos\theta_{11}\cos\theta_{16}\right)$$
$$M_{23}=-\sin\theta_{11}\cos(\theta_{14}+\theta_{15})$$
$$M_{24}=R\begin{pmatrix}\cos\theta_{17}\left(\sin\theta_{11}\cos\theta_{16}\sin\left(\theta_{14}+\theta_{15}\right)+\cos\theta_{11}\sin\theta_{16}\right)\\-\sin\theta_{17}\left(\sin\theta_{11}\sin\theta_{16}\sin\left(\theta_{14}+\theta_{15}\right)-\cos\theta_{11}\cos\theta_{16}\right)\end{pmatrix}+L_4\sin\theta_{11}\sin\theta_{14}$$
$$-L_7\sin\theta_{11}\cos\left(\theta_{14}+\theta_{15}\right)$$
$$M_{31}=\cos\theta_{16}\cos\theta_{17}\cos(\theta_{14}+\theta_{15})$$
$$-\sin\theta_{16}\sin\theta_{17}\cos(\theta_{14}+\theta_{15})$$
$$M_{32}=-\cos\theta_{16}\sin\theta_{17}\cos(\theta_{14}+\theta_{15})$$
$$-\sin\theta_{16}\cos\theta_{17}\cos(\theta_{14}+\theta_{15})$$
$$M_{33}=\sin(\theta_{14}+\theta_{15})$$
$$M_{34}=R\left(\cos\theta_{16}\cos\theta_{17}\cos\left(\theta_{14}+\theta_{15}\right)-\sin\theta_{16}\sin\theta_{17}\cos\left(\theta_{14}+\theta_{15}\right)\right)+L_7\sin\left(\theta_{14}+\theta_{15}\right)$$
$$+L_3+d_{12}+L_{14}\cos\theta_{14}$$

The pose matrix of the moving coordinate system o-xyz relative to the fixed coordinate system O-XYZ can be represented by the Z-Y-X Euler angle (α,β,γ) matrix, and the degree of freedom of the 2-CRS-S ' mechanism is 2, then the Z-axis rotation angle α= 0, the pose matrix is :

$$T=\begin{bmatrix}\cos\beta & \sin\beta\sin\gamma & \sin\beta\cos\gamma & x\\ 0 & \cos\gamma & -\sin\gamma & y\\ -\sin\beta & \cos\beta\sin\gamma & \cos\beta\cos\gamma & z\\ 0 & 0 & 0 & 1\end{bmatrix} \quad (9)$$

In the formula : T is the pose matrix ; x, y, z are the position coordinates of the origin o of the moving coordinate system in the fixed coordinate system O-XYZ ; β and γ are the rotation angles of the moving platform around the OY axis and the OX axis in the fixed coordinate system.

The transformation matrix ${}^{O}_{o}T$ from the dynamic coordinate system o-xyz to the fixed coordinate system O-XYZ is equal to the pose matrix T of the dynamic coordinate system relative to the fixed coordinate system, that is :

$${}^{O}_{o}T=T \quad (10)$$

By making the elements of the corresponding positions in the two matrices equal one by one, the corresponding equations can be established, and the equations can be solved. The expression of each variable is calculated, that is, the inverse solution of the attitude of the branched chain is obtained. The result is :

$$\theta_{11}=arctan\frac{-\sin\gamma}{\sin\beta\cos\gamma} \quad (11)$$

$$\theta_{14}=arcsin\left(\frac{x-R\begin{pmatrix}\sin^2\left(arctan\frac{-\sin\gamma}{\sin\beta\cos\gamma}\right)\cos\beta+\cos^2\gamma\cos\beta\\-\sin^2\left(arctan\frac{-\sin\gamma}{\sin\beta\cos\gamma}\right)\cos^3\beta\cos^2\gamma\end{pmatrix}+R}{\frac{+L_7\cos\left(arctan\frac{-\sin\gamma}{\sin\beta\cos\gamma}\right)\cos(arcsin(\cos\beta\cos\gamma))}{L_4\cos\left(arctan\frac{-\sin\gamma}{\sin\beta\cos\gamma}\right)}}\right)(\beta\neq0) \quad (12)$$

$$\theta_{15}=arcsin({}_{\cos}\beta\cos\gamma)-\theta_{14} \quad (13)$$

$$\theta_{16}+\theta_{17}=\arccos\left(\frac{\frac{\cos\gamma}{\cos\left(\arctan\frac{-\sin\gamma}{\sin\beta\cos\gamma}\right)}+\sin\left(\arctan\frac{\sin\gamma}{\sin\beta\cos\gamma}\right)\frac{\sin\gamma\cos^2\beta}{\sin\beta}}{}\right) \quad (14)$$

$$=\arcsin\left(\cos\beta\sin\left(\arctan\frac{\sin\gamma}{\sin\beta\cos\gamma}\right)\right)$$

$$d_{12}=\mathrm{z}-L_3-L_4\cos\theta_{14}+R\sin\beta-L_7\cos\beta\cos\gamma \quad (15)$$

Similarly, the inverse solution expression of another driving branch chain can be obtained.

4. Positive solution analysis of motion based on particle swarm optimization algorithm

In this paper, the particle swarm optimization algorithm in the numerical algorithm is used to solve the positive solution of the mechanism. By constructing the optimal solution equation, the positive solution of the parallel mechanism is transformed into the optimal solution. The calculation process is as follows.

(1) Determination of optimization objective function

Combined with the inverse attitude equation of the two driving branches, the optimization function equation is obtained as follows:

$$f_{1=\mathrm{Z}}-L_3-L_4\cos\theta_4+R\sin\beta-d_{12} \quad (16)$$

$$f_{2=\mathrm{Z}}-L_3-L_4\cos\theta_4-R\frac{\sqrt{3}\cos\beta\sin\gamma+\sin\beta}{2}-d_{22} \quad (17)$$

In the formula, z is the distance from the origin o of the moving coordinate system to the origin O of the fixed coordinate system; L_3, L_4, R and L_7 were fixed parameters. β and γ are the deflection angles of the moving platform around the OX axis and the OY axis, respectively; d12 and d22 are the displacement of the push rod in the two driving branches (driving input).

(2) Accuracy function

In order to ensure that the optimization solution has high accuracy, let F=|f1|+|f2| be the accuracy function of the particle. When $F<10^{-4}$, the optimization algorithm stops iteration and outputs the optimal solution.

(3) Initialize PSO parameters [12]

The velocity update formula and position update formula of particle swarm optimization are :

$$V_i^{\,d}=\omega\cdot V_i^{\,d}+c_1\cdot rand_1^d\cdot\left(pbest_i^d-x_i^d\right)+c_2\cdot rand_2^d\cdot\left(gbest_2^d-x_i^d\right) \quad (18)$$

In the formula, the first part is the inertia term, which is the inertia weight to balance the global and local search capabilities in the optimization algorithm. The relatively large is conducive to the exploration and jump out of the particle population, and the relatively small is conducive to the convergence and development of the particle population [12] ; the second part is the ' self-cognition ' term, which is used to represent the attraction of pbesti to individual particles in the population, c1 is the acceleration coefficient, also known as the learning factor, and rand1 represents a random number generated in the range of [0,1]. The third part is the ' social cognition ' item, in which gbest will communicate with each particle individual in the population and share global information, so that each particle individual has the possibility of approaching the global optimal solution, c2 and rand2 are consistent with c1 and rand1 in the second part.

Various parameters need to be set at the beginning of the algorithm operation, as shown in Table 2. Five groups of different parameters are input, and the output results are shown in table 3.

Taking the given input parameter (displacement) into the optimized particle swarm optimization algorithm, the rotation angle of the moving platform around the OY and OX axes can be calculated, as shown in Table 3:

Table.2 Particle swarm optimization algorithm parameters

Parameter	Numerical value
Study factor	2
Inertia weight	0.8
Spatial dimensions	2
Population size	100
Maximum number of iterations	500
Value ranges of β	[-10,10]
Value ranges of γ	[-10,10]

Table.3 Forward optimization solution results of driving branch chain

numerical example	input		output	
	d12/mm	d22/mm	β/°	γ/°
1	2	-1	1.9186	0
2	1.4142	0.5176	1.3564	-1.3564
3	0	1.732	0	-1.9185
4	-1.4142	1.9318	-1.3561	-1.3567
5	-2	1	-1.9169	0
6	-1.4142	-0.5177	-1.3561	1.3561
7	0	-1.7321	0	1.979
8	1.4142	-1.9319	1.3564	1.3558

5. Adams Motion Simulation Analysis

The three-dimensional model of 2-CRS-S' mechanism is established in SolidWorks software, and it is imported into Adams software. The corresponding kinematic pair constraints are added, and the corresponding drive and Step functions are added to the mechanism drive pair. After clicking the simulation, the kinematics simulation analysis of the mechanism is carried out. After the simulation, the kinematics simulation data of the end actuator can be obtained in the results.

The Step function is used as the driving mode of the two drives. The simulation time of the mechanism is set to 4s, and the step size is 500. After the kinematics simulation is completed, the displacement curve of the driving branch is obtained as shown in Fig. 6. The rotation angle curve of the moving platform around the Y axis and the X axis is shown in Fig. 7.

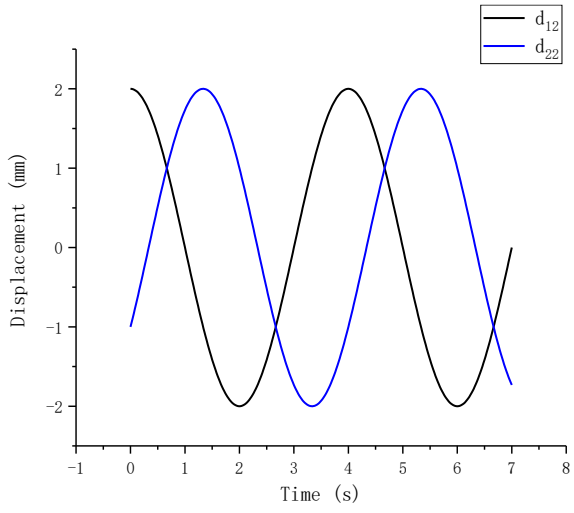


Fig.6 Displacement curve of driving branch chain actuator

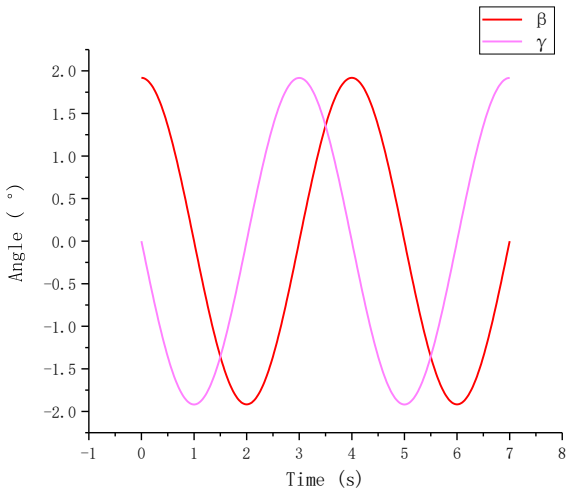


Fig.7 Moving platform deflection angle curve

It can be seen from Fig.6 and Fig.7 that when the displacement of the moving platform of the parallel mechanism changes according to the sine law, the rotation angle curve of the moving platform around the Y axis and the X axis is a continuous smooth curve, and the change period and amplitude of the two curves are the same, indicating that the mechanism moves smoothly during operation and the driving performance of the mechanism is good.

6. Conclusion

In this paper, a 2-CRS-S' parallel mechanism with two rotational degrees of freedom is taken as the research object. The structural parameters of the mechanism are analyzed by D-H matrix method, and the inverse solution expression of its attitude is obtained. After that, the PSO particle swarm optimization algorithm is used to optimize the attitude positive solution of the mechanism. Finally, the kinematics simulation of the 2-CRS-S' parallel mechanism is carried out in Adams software, and the angle and angular velocity curves of the mechanism during operation are obtained. By analyzing the obtained curves, it can be seen that the mechanism runs smoothly during the movement and has good kinematic performance.

References

[1] TIAN Hai-bo, MA Hong-wei, XIA Jing, et al. Stiffness Analysis of a Metamorphic Parallel Mechanism with Three Configurations[J]. Mechanism and Machine Theory, 2019, 142(18): 252 —256.

[2] Zhu Dongsheng, Guo Zhongfeng, Zhao Wenzeng et al.4-SPS / UPU parallel mechanism kinematics analysis [J]. Yi-zhong Technology, 2022 (02) : 17-20 + 25.

[3] CHEN Wenbo, CHEN Weijie et al. Dynamic modeling and simulation of 2UPR / UPS / UP parallel mechanism [J]. Journal of Shanghai University of Technology, 2022, 36 (03) : 309-314.

[4] Shang Mingming, Wang Heng, Shi Baoyu et al. RSR dynamic modeling and simulation of parallel mechanism [J].Journal of Tangshan Normal University, 2022,44 (06) : 32-36.

[5] Guo Dingxu et al. Dynamic Modeling and Model-Based Control with Neural Network-Based Compensation of a Five Degrees-of-Freedom Parallel Mechanism[J]. Machines, 2023, 11(2) : 195-195.

[6] Zou Yupeng et al. Design and Experimental Research of 3-RRS Parallel Ankle Rehabilitation Robot. [J]. Micromachines, 2022, 13(6) : 950-950.

[7] Du Xiaoqiang et al. Design and optimization of solar tracker with U-PRU-PUS parallel mechanism[J]. Mechanism and Machine Theory, 2021, 155: 104107.

[8] Liwei Yang et al. Parameter Calibration of 6-Degree-of-Freedom Parallel Mechanism Based on Orthogonal Displacement Measuring System[J]. Optik, 2020, : 165806-.

[9] Hongzhou Wang et al. Dynamics analysis of a novel two-translation parallel mechanism[J]. Vibroengineering PROCEDIA, 2020, 33: 193-198.

[10] Cai Jie et al. Modeling Method of Autonomous Robot Manipulator Based on D-H Algorithm[J]. MOBILE INFORMATION SYSTEMS, 2021

[11] Bao-qiang Tian and Jian-cheng Yu and Ai-qun Zhang. Dynamic modeling of wave driven unmanned surface vehicle in longitudinal profile based on D-H approach[J]. Journal of Central South University, 2015, 22(12): 4578-4584.

[12] Li Panchi, Wang Haiying, Yang Yu. A stochastic particle swarm optimization algorithm and its application [J].Computer system application, 2012,21 (02) : 245-248 + 217.